
Estimating the history of mutations on a phylogeny

Jonathan P. Bollback, Paul P. Gardner, and Rasmus Nielsen

6.1 Introduction

Evolution is a historical process that has left its signature on the molecules and morphology of living organisms. Attempts to better understand the specific and general features of evolution involve making inferences about the past from these tell-tale signs (Felsenstein, 1985; Brooks and McLennan, 1991; Harvey and Pagel, 1991; Pagel, 1999). Ancestral state reconstruction is a powerful tool in this endeavor, as exemplified by its application to a wide array of questions (e.g. Langley and Fitch, 1974; Gillespie, 1991; Templeton, 1996; Messier and Stewart, 1997; Bishop *et al.*, 2000). Traditionally, ancestral reconstruction has relied on well-understood approaches such as parsimony. However, the last decade has seen an excited flurry of research into statistical approaches as exemplified by the contents of this volume and the primary literature.

In a general sense, most methods for ancestral reconstruction have focused on reconstructing the ancestral states at the internal nodes of a phylogeny. Often we are not interested in particular nodes of the phylogeny but the whole history of a character. In this chapter we focus on a Bayesian method for estimating these histories on phylogenies (we refer to a complete description of a character's history as its mutational path). Mutational path methods differ most notably from other approaches in their ability to estimate not only the ancestral states at the internal nodes of a phylogeny but also the order and timing of mutational changes on the phylogeny. Our goal here is to provide a concise introduction to the statistical

tools necessary for estimating mutational histories and making inferences from these histories, and to provide some examples of the power of this recent approach.

6.2 Likelihood and Bayesian methods

Estimation of ancestral character states using maximum likelihood proceeds from a straightforward extension of the usual algorithm for calculation of the likelihood function in phylogenetics. Let $f_{ij}(k)$ be the fractional probability of nucleotide k at site i for node j of the phylogeny. That is, $f_{ij}(k)$ is the probability of all the data in site i below node j given that the ancestral state at node j is k . The maximum-likelihood estimate of ancestral state in node j is then obtained by placing the root at node j and maximizing

$$L(k) = f_{ij}(k) \tag{6.1}$$

with respect to k . Other parameters of the evolutionary model (branch lengths, parameters of the mutational model, etc.) have typically been estimated prior to the analysis and are assumed to be fixed. The method can also be extended to find the joint set of ancestral states for all nodes that maximizes the likelihood (Yang *et al.*, 1995; Koshi and Goldstein, 1996; Pupko *et al.*, 2000). For more details on maximum-likelihood estimation, please see other relevant chapters of this volume. One important thing to notice is that under a uniform prior for all possible ancestral states, the maximum-likelihood estimate is also a Bayesian maximum *a posteriori* probability (MAP) estimate.

However, from a Bayesian perspective it arguably makes little sense to first estimate all parameters of the model (except ancestral states) using maximum likelihood, and then to estimate ancestral states. Instead, it is preferable to estimate ancestral sequences jointly for all sites at the same time while integrating over all other parameters. The advantage is that the phylogenetic uncertainty, and uncertainty regarding the parameters of the evolutionary model, are taken into account in the estimation of ancestral states. This is achievable using Markov chain Monte Carlo (MCMC) methods described in the following section. One advantage of this method is that it directly provides an estimate of an entire evolutionary history; that is, of ancestral states, not only at the nodes of the phylogeny, but also at any point in time along the branches (edges) of the phylogeny.

6.3 MCMC

The basic idea in the MCMC algorithm is to represent mutations directly on the phylogeny. A history of mutations along one or more branches of the phylogeny is called a mutational path. The concept of a mutational path is illustrated in Figure 6.1. Bayesian ancestral reconstruction using MCMC exist in two flavors: (1) a two-step approach where a sample of genealogies and

parameter values is first sampled using MCMC, and mutational paths are subsequently simulated given particular sampled phylogenies (Nielsen, 2002; Bollback, 2006), and (2) direct methods where the mutations are represented on the phylogeny while simulating the genealogy (Nielsen, 2001). Both approaches achieve the same goal, but they differ in computational efficiency and in which models they can accommodate. In general, we will assume the model of evolution can be described by a Markov chain on a finite, discrete state space with known generator, such as the set of all possible amino acids, all possible codons, or all possible nucleotides. We will also initially assume that this Markov process is independent among sites, although, as we will show, one of the advantages of these methods is that they can easily be extended to models of correlated evolution among sites.

6.3.1 Sampling mutational paths

In the following we will describe how algorithms of type 1 proceed. Consider first the case of a fixed phylogeny with known branch lengths and evolutionary model. We will first describe how to sample a mutational path stochastically under a particular evolutionary model. From eqn 6.1 we see that,

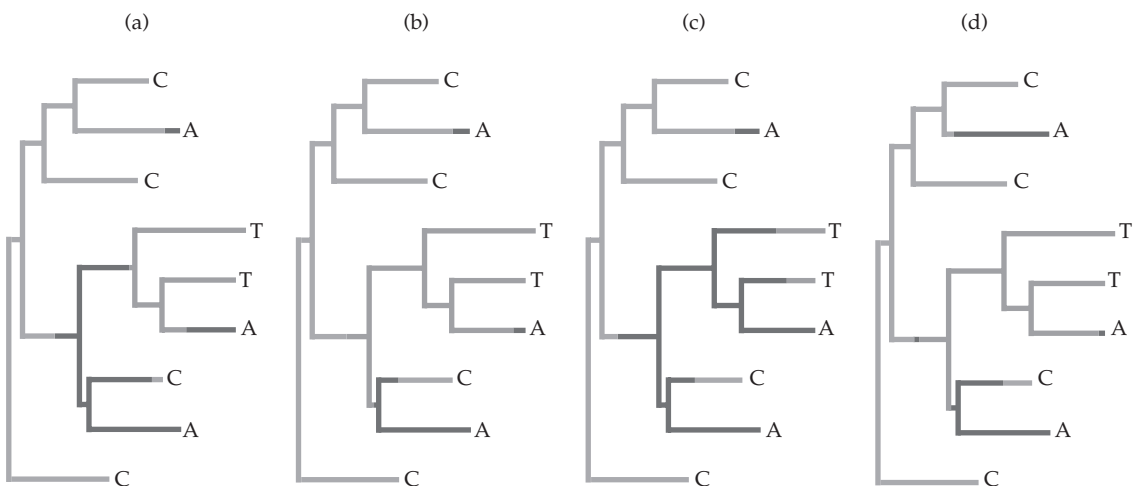


Figure 6.1 Examples of four mutational paths for a single site. Mutational paths were produced using the SIMMAP software package (Bollback, 2006).

$$P(y_{ij} = k | x_i) = \frac{f_{ij}(k)\pi(k)}{\sum_b f_{ij}(b)\pi(b)} \quad (6.2)$$

where π_b is the prior probability of state b (usually assumed to be the stationary frequency of b under the model), x_i is the observed data in site i , and y_{ij} is the unknown ancestral state in site i , node j . The ancestral state at the root of the tree can then be sampled according to these probabilities. At a child node of node j , say node h , the ancestral state, y_{ih} , can then be sampled according to the probabilities

$$P(y_i = k | x_i, y_{ij} = v) = \frac{f_{ih}(k)p_{vk}(h)}{\sum_b f_{ih}(b)p_{vb}(h)} \quad (6.3)$$

This sampling procedure can then be repeated recursively along the branches in the tree until ancestral sequences have been sampled for all nodes. In a sample of n sequences the resulting vector of nucleotides, $y_i = (y_{i1}, y_{i2}, \dots, y_{i(2n-3)})$, represents a sample from $P(y_i, x_i)$.

For a time-reversible model of substitution, the distribution of y does not depend on where in the tree the root has been placed. An entire mutational path can then be obtained by sampling paths conditional on the ancestral sequences at the nodes. If we let z_{ih} be the mutational path leading to node h from node j for site i , with sampled ancestral states $y_{ih} = k$ and $y_{ij} = v$, a sample from the density $p(z_{ih} | y_{ih} = k, y_{ij} = v)$ can be obtained using standard methods for simulating Markov chains starting at state v . The conditioning can be achieved by simply eliminating paths which do not end in state k , and can be sped up in various ways. Repeating this scheme for all branches of the tree provides a full sample of $z_i | y_i$. The simulation procedure is completed by applying this procedure to all sites, providing a full sample of $z = (z_1, z_2, \dots)$ and $y = (y_1, y_2, \dots)$.

6.3.2 Incorporating phylogenetic uncertainty

The preceding description of the simulation procedure assumes that the phylogenetic tree and the parameters were known; that it produces samples from the density $p(z, y | x, \theta)$, where θ is a vector of all the nuisance parameters, including the

mutational model and the phylogenetic tree with branch lengths. However, usually θ will not be known. In such cases, we wish to be able to obtain samples from

$$p(z, y | x) = \int p(z, y | x, \theta) p(\theta, x) d\theta \quad (6.4)$$

where the integral is over all supported values of θ . We can think of this integral as a sum over all topologies of the tree and a multiple integral over all possible branch lengths and parameters of the mutational process. The representation in eqn 6.3 suggests the following method for obtaining samples from $p(z, y | x)$:

- 1 sample $\theta^{(1)}, \theta^{(2)}, \dots, \theta^{(n)}$ from $p(\theta | x)$
- 2 sample $z^{(s)}, y^{(s)}$ from $p(z, y | x, \theta^{(s)})$ for $s = 1, 2, \dots, n$.

The samples from $p(\theta | x)$ can be obtained using any of the well-known MCMC programs, for example MrBayes (Huelsenbeck and Ronquist, 2001). This method provides a method for obtaining samples from $p(z, y | x)$ which takes advantage of existing computational methods for Bayesian inference in phylogenetics and is comparatively easy to implement.

6.3.3 Direct methods

In the direct methods (Nielsen, 2001; Robinson *et al.*, 2003) the MCMC procedure is applied directly to a phylogeny with mutational paths; the state space of the Markov chain is the set of supported values of (y, z, θ) . A Markov chain with stationary density $p(y, z, \theta | x)$ can be simulated, for example, by iterating updates of (x, y) : for $i = 1, 2, \dots, B$, where B is the number of sites:

- 1 simulate a new value of (z_i, y_i) , (z_i^*, y_i^*) , from a proposal density $q(y_i^*, z_i^* | x_i, \theta)$;
- 2 accept (z_i^*, y_i^*) with probability $(p(y_i^*, z_i^* | x_i, \theta) q(y_i, z_i | x_i, \theta)) / (q(y_i^*, z_i^* | x_i, \theta) p(y_i, z_i | x_i, \theta))$.

and updates of θ :

- 1 simulate a new value of θ , θ^* from a proposal density $q(\theta^* | x, y, z)$;
- 2 accept θ^* with probability $(p(x, y, z | \theta) q(\theta | x, y, z) p(\theta^*)) / (q(\theta^* | x, y, z) p(x, y, z | \theta) p(\theta))$.

In the above notation, the current state before an update is simply denoted by (x, y, θ) to simplify the

notation and (z^*, y^*) is (z, y) , with (z_i^*, y_i^*) replacing (z_i, y_i) . Notice that any update kernel $q(\dots)$ can be used as long as it ensures that all values of (θ, z, y) supported by $p(\theta, z, y|x)$ eventually can be reached. This simulation procedure takes advantage of the fact that $p(c, x|\theta)$ easily can be calculated directly from the generator as the sampling path of a continuous-time Markov chain without the need to calculate time-dependent transition probabilities. However, this MCMC procedure can be slow to converge because of the correlation between (y, z) and θ . One of the advantages of this procedure is that it allows the use of models with correlated evolution among sites (e.g. Robinson *et al.*, 2003; Yu and Thorne, 2006). In models of protein evolution involving tertiary structure, or models involving CpG hypermutations, the state space of the Markov model is the set of 4^B possible sequences of length B . However, the likelihood function can no longer be written as the product of the likelihood in multiple independent sites. This means that the conventional statistical methods for inference are inapplicable. Numerical calculation of the time-dependent transition probabilities of the process are hard or impossible to calculate and methods based on summing over all possible states (e.g. as part of the likelihood calculation) are intractable. However, whereas it is not possible to calculate $p(x|\theta)$ in these models, calculations of $p(x, y, z|\theta)$ are straightforward. This means that MCMC procedures with state space on (y, z, θ) can be implemented relatively easily.

6.4 Statistical inference using sampled mutational paths

After obtaining samples from the posterior distribution of (y, z, θ) using either of the two methods, inference in a Bayesian framework proceeds in a straightforward fashion. The posterior expectation (or summary statistic) of any function of the mutational path can easily be calculated. For example, Nielsen (2001) used this method to calculate the posterior expectation of the ages of non-synonymous and synonymous mutations occurring on a phylogeny. The framework provides a computationally tractable framework for making rigorous statistical inferences based on

mutational paths. Bollback (2002) and Nielsen and Huelsenbeck (2001) showed how statistical measures of uncertainty can be obtained in this framework based on the posterior predictive distribution.

Briefly, the posterior predictive distribution measures uncertainty by estimating the “null” or predictive distribution of mutational paths, given the information obtained from the posterior distribution. In this way, a summary statistic can be compared with its predictive distribution to test hypotheses and measures of statistical uncertainty. This approach is appealing because it can be applied and tailored to a wide variety of questions involving only the ability to specify a summary statistic and simulate posterior predictive mutational histories. A typical summary statistic would be calculated by summing over simulated mutational mappings and taking the expectation

$$h(x) = \frac{1}{N} \sum_i h(x, y^{(i)}, z^{(i)}) \quad (6.5)$$

Using the indirect approach for obtaining samples from the posterior distribution, the estimation of the posterior predictive distribution can be accomplished in the following way.

- 1 Generate n samples of $\theta, (\theta^{(1)}, \theta^{(2)}, \dots, \theta^{(n)})$ from the posterior distribution using established MCMC methods.
- 2 For $j = 1, 2, \dots, n$ simulate a new set of aligned sequence, $x^{(j)}$, under $\theta^{(j)}$; simulate $k \leq n$ mutational paths, $(z^{(j,i)}, y^{(j,i)})$, $i = 1, 2, \dots, k$, based on $x^{(j)}$ and $\theta^{(j)}$.
- 3 The distribution of $h(x_{(j)}) = \sum_i h(x, y^{(j,i)}, z^{(j,i)})$ then approximates the posterior predictive distribution of $h(x)$.

It should be noticed that for each of the simulated predictive data sets the posterior predictive expectation of a site’s mutational history is averaged over all of the samples from the posterior. In this way we can effectively integrate out uncertainty in the posterior distribution using a single MCMC run. For additional details on predictive distributions the reader is referred to the literature (e.g. Nielsen and Huelsenbeck, 2001; Bollback, 2002; Suchard *et al.*, 2003).

6.5 Examples

The method of mutational mapping has already found wide use in addressing questions about the age of mutations (Nielsen, 2001), positive selection (Nielsen and Huelsenbeck, 2001), morphological evolution (Huelsenbeck *et al.*, 2003), and modeling non-independence among residues (Dimmic *et al.*, 2005; Yu and Thorne, 2006), among others.

In this section we will illustrate two different uses of mutational mapping. Each of the analyses were performed using the SIMMAP software package (a brief introduction to this package is provided in the next section). We hope that this section will demonstrate the types of question that can be addressed using mutational mapping and motivate its use and further development.

6.5.1 Characterizing transmembrane regions of proteins

Transmembrane proteins span cellular membranes with intra- and extramembrane regions. One feature of these proteins is the highly hydrophobic (water-fearing) nature of the helices spanning the membrane and the hydrophilic (water-loving) nature of the protein domains in the cytoplasmic and periplasmic spaces. An early single-sequence approach evaluated the hydropathy of the primary structure of a protein (Kyte and Doolittle, 1982). This approach plots hydropathy, using a sliding window spanning n residues, as a function of sequence position (residue), which have been called Kyte–Doolittle hydropathy plots.

The Kyte–Doolittle method considers only a single sequence. To demonstrate the use of mutational maps we present an approach that produces a comparative Kyte–Doolittle plot that accommodates multiple sequences, uncertainty in the phylogeny relating the sequences, and the evolutionary model describing changes in those sequences. Whereas more advanced methods exist for discovering transmembrane domains (e.g. Krogh *et al.*, 2001), the simple approach described here offers the ability to summarize data across multiple sequences to initially identify likely transmembrane regions. In addition, other

methods may benefit from the inclusion of this type of a multi-sequence approach.

Two data-sets are analyzed using the indirect mutational mapping approach: a primate cytochrome oxidase II data set (Yoder and Yang, 2004) consisting of 52 species of lemur; and a primate chemokine receptor CCR5 data-set (a subset of sequences analyzed by Mummidi *et al.* (2000)) consisting of the mouse sequence and 11 primate sequences.

Cytochrome oxidase II is one of a number of proteins involved in the electron-transport chain in mitochondria. Cytochrome oxidase II has two transmembrane domains (TM1 and TM2; see Figure 6.2) and a highly aromatic (hydrophilic) region of amino acid residues involved directly in electron transport (Adkins and Honeycutt, 1994). Using the mapping approach the hydropathy of each site, averaged across the probable phylogenies, was evaluated for the primate cytochrome oxidase II. Sampling estimates of the phylogeny and model were first obtained using MrBayes (Huelsenbeck and Ronquist, 2001). SIMMAP was used to map mutational paths for each codon and from these the history of the hydropathy was summarized. This approach weights a site's hydropathy by taking the branch-length-weighted sum of the site's amino acid mutational history. The tree-weighted posterior expectation of hydropathy for each residue was evaluated across 105 trees and was plotted in a Kyte–Doolittle plot with a sliding window of size 11 (see Figure 6.2). The method clearly identifies the two transmembrane regions of cytochrome oxidase II protein and identifies the conserved hydrophilic region with amino acid residues involved directly in electron transport.

The second data-set consisted of 11 primate sequences and the mouse sequence (Mummidi *et al.*, 2000), which were retrieved and aligned from the GenBank Nucleotide Sequence Database; mouse, human, chimpanzee, gorilla, green monkey, spider monkey, squirrel monkey, golden lion tamarin, golden-rumped tamarin, a marmoset, and two species of lemur. The chemokine receptor (CCR5) protein is a coreceptor target of HIV and SIV, and possibly other related viruses (Mummidi *et al.*, 2000; Paterlini, 2002). CCR5 has seven

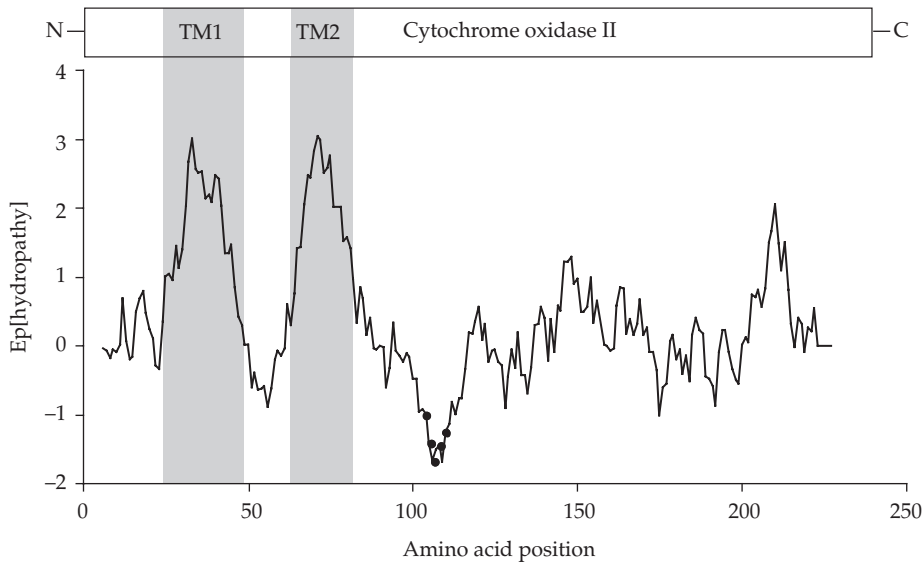


Figure 6.2 A comparative Kyte–Doolittle hydropathy plot of the hydrophobic character of the primate cytochrome oxidase II protein using mutational mapping to summarize multiple sequences. The location of the transmembrane (TM) domains are shown at the top and the circles show the predicted amino acids involved in electron transport.

transmembrane domains, labeled TM1–TM7 (Paterlini, 2002). Using mutational histories we analyzed CCR5 for the hydrophobic signature of the transmembrane regions (Figure 6.3) and the association between hydrophobic change and positive selection (Figure 6.4). In addition, for each site we calculated the posterior expectation of the change in hydrophobicity.

Of the seven transmembrane domains in CCR5 TM1–TM6 are clearly identified as having had a highly hydrophobic history, whereas TM7 does not show a large deviation in its hydrophobicity. The cytoplasmic/periplasmic regions show a considerable bias towards being hydrophilic. Inspection of the mean change in hydrophobicity indicates that there is a general pattern of transmembrane regions showing values close to 0 or slightly negative, whereas hydrophilic regions exhibit larger changes with a tendency towards hydrophobicity (Figure 6.4). This latter observation at first seems surprising but may reflect tertiary packing in these regions in which evolution is occurring at mostly buried residues or at residues that are under selection for interaction with other proteins; sites that show evidence for positive

selection occur, predominantly, in cytoplasmic/periplasmic domains (74% of sites; Figure 6.4). In addition, sites in transmembrane regions that show evidence for positive selection show a large tendency for change to more hydrophobic residues. Nevertheless the approach provides comparative information indicating domains that are likely to have had a highly hydrophobic mutational history and, thus, likely to be transmembrane regions.

6.5.2 Nucleotide covariation in mitochondrial tRNAs

One powerful use of the mutational mapping approach is in detecting non-independence, or covariation, among nucleotide residues. Mutational histories have been successfully applied to detecting compensatory changes in amino acid residues (Dimmic *et al.*, 2005) and correlation between morphological characters (Huelsenbeck *et al.*, 2003).

To illustrate the use of mutational histories for detecting nucleotide covariation we analyzed all 21 mitochondrial tRNAs for 106 species with the hope

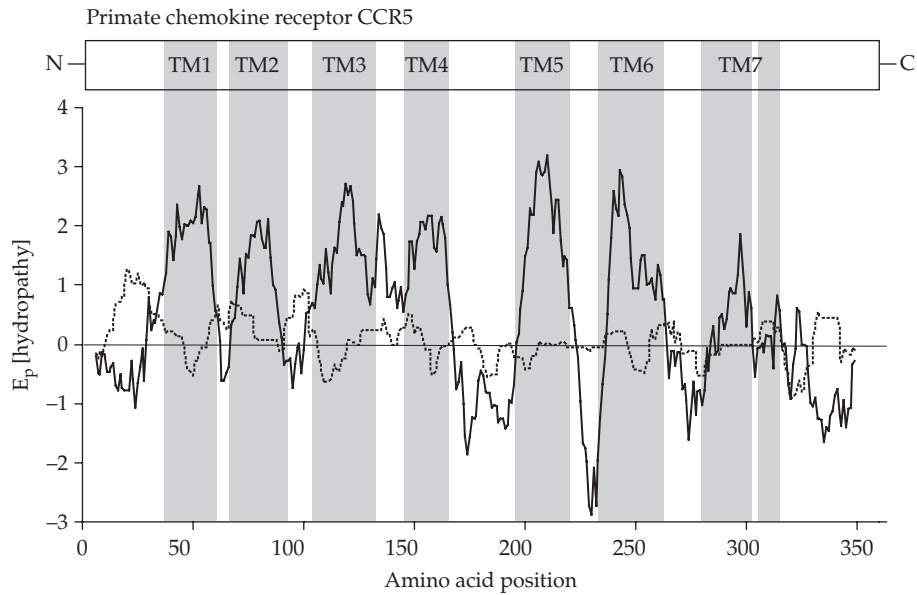


Figure 6.3 A comparative Kyte–Doolittle hydropathy plot of the hydropathic features of the primate CCR5 protein using mutational mapping to summarize multiple sequences. The posterior expectation of hydropathy along the gene is shown by the black line while the dashed line is the posterior expectation of the direction and magnitude of change in hydropathy (see Figure 6.4 for a plot of the hydropathic magnitude and direction of changes on a residue-by-residue basis). The plots were generated using a window size of 11 residues. Locations of the transmembrane (TM) regions are shown at the top.

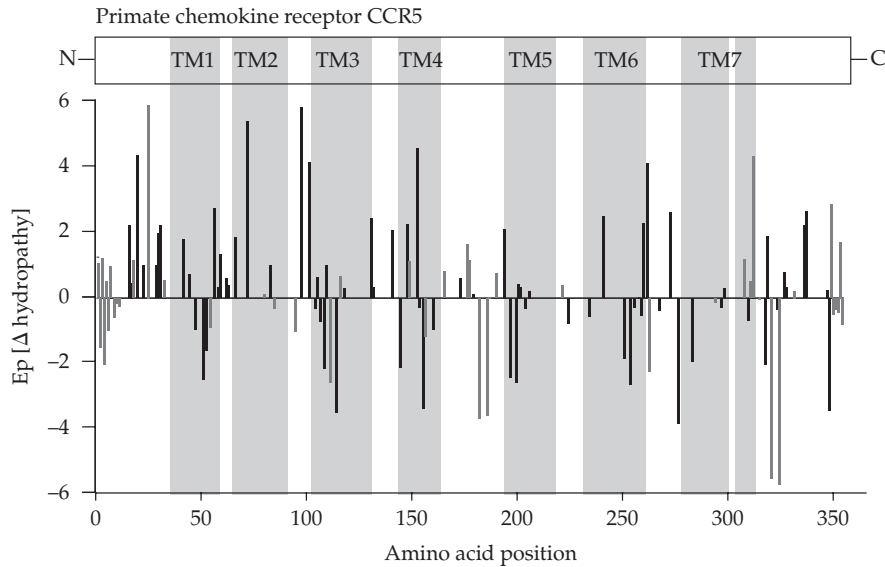


Figure 6.4 Patterns of change in hydropathy and positive selection. The magnitude and direction of change in hydropathy are plotted along the sequence. Sites that show at least two substitutions and with a non-synonymous/synonymous ratio >1 are shown in gray.

of detecting positive evidence for covariation among base-pairing residues. As above, we adopted the indirect approach using MrBayes (Huelsenbeck and Ronquist, 2001) to provide a sampling approximation of the phylogeny and substitution model parameters. All 21 tRNA genes were concatenated and the GTR + gamma substitution model was used (Lanavé *et al.*, 1984; Yang, 1994) to obtain samples from the posterior distribution of the phylogeny and substitution model parameters.

But how can we measure covariation among nucleotides using mutational histories? The answer is straightforward. For each site we sample a mutational path and then compare the covariation (coincidence of states) between each site's history. Any number of statistics can be used. To evaluate the degree of covariation we calculated the association between different states along each branch of a phylogeny using the following statistic:

$$m_{ij} = f_{ij} \log_2 \frac{f_{ij}}{f_i f_j} \quad (6.6)$$

where f_{ij} is the fraction of time state i is associated with j in a character history, and f_i is the fraction time in a particular state independent of associations (i.e. the sum of time spent in a particular state on the phylogeny). We refer to this statistic as the mutual historical information content, or MHIC, because of its relationship in form to the

classical mutual information content statistic (Chiu and Kolodziejczak, 1991; Gutell *et al.*, 1992). By averaging over all state associations we get the following statistic for the overall character correlation:

$$M = \sum_{i=1}^x \sum_{j=1}^y m_{ij} \quad (6.7)$$

In addressing whether we can detect covariation in RNA molecules, which is the result of base-pairing constraints, we perform the summation over only Watson–Crick (AU and GC) and wobble pairs (GU). In this way we focus on covariation that is due to base-pairing. To accommodate uncertainty in the phylogeny and substitution model parameters we calculated the posterior expectation of the MHIC statistic for each pair and then compared the known pairs with the unknown pairs for each tRNA. A comparison of the MHIC reveals that paired sites show a strong signature of covariation relative to unpaired sites (Figure 6.5) in 20 of the 21 tRNAs; in the single case of the tRNA_{Met} the difference between paired and unpaired is indistinguishable. This is likely the result of very little variation in the tRNA_{Met} at paired sites. These results clearly indicate that the signature of covariation can be easily identified using the mutational history approach.

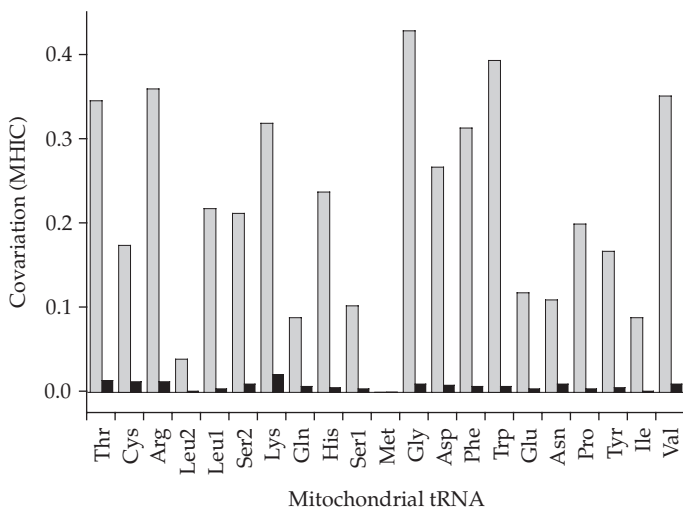


Figure 6.5 Nucleotide covariation measures for the 21 mammalian tRNAs. Gray bars represent the mean mutual historical information content (MHIC) for known pairs and black bars show the means of unpaired sites. A comparison of the standard deviations (not shown) indicates that in all but the tRNA_{Met} these differences are significant.

Whereas the previous results indicate a strong difference in the signature of covariation between known pairs and unpaired sites we might wish to determine how well the method predicts true pairs (true positives) relative to mis-assigning pairs (false positives). One commonly used measure is Mathew's correlation coefficient (MCC):

$$\text{MCC} = \frac{TP \times TN - FP \times FN}{\sqrt{(TP+FP)(TP+FN)(TN+FP)(TN+FN)}} \quad (6.8)$$

where TN is the number of true negatives, TP is the number of true positives, FN is the number of false negatives, and FP is the number of false positives. In using this measure the first step is to rank each comparison MHIC value and then to break this into discrete intervals or thresholds.

Values above the threshold are considered to be *paired* and values below to be *unpaired*. At each threshold the MCC is calculated and is a measure of the method's ability to correctly identify true pairs while minimizing false positives. Figure 6.6 shows the MCC values for the the tRNA_{Gly} and tRNA_{His} .

We evaluated overall performance by calculating the mean and 95% confidence intervals of MCC at each threshold value for all 21 tRNAs (Figure 6.7). The performance of the method, as measured by the MCC, is high, with a maximum mean MCC value of 0.42 averaged across the 21 tRNAs, and with 11 out of 21 (52%) of the tRNAs with individual maximum MCC values above 50%. The performance of this approach does decline with divergence as expected (data not shown).

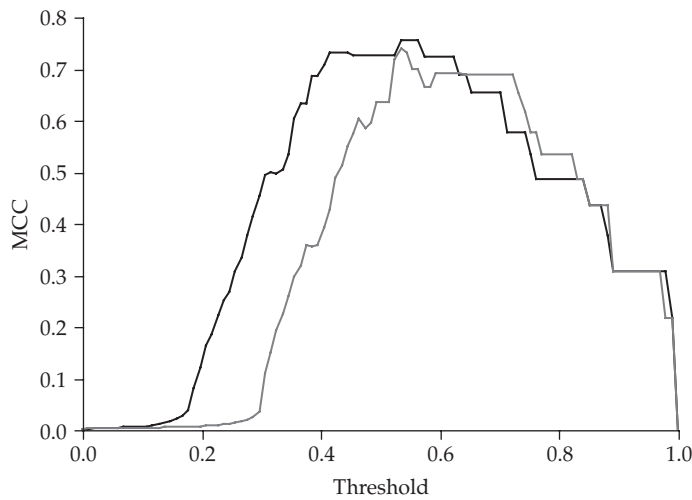


Figure 6.6 Mathew's correlation coefficient (MCC) for the mammalian tRNA_{Gly} (black) and tRNA_{His} (gray).

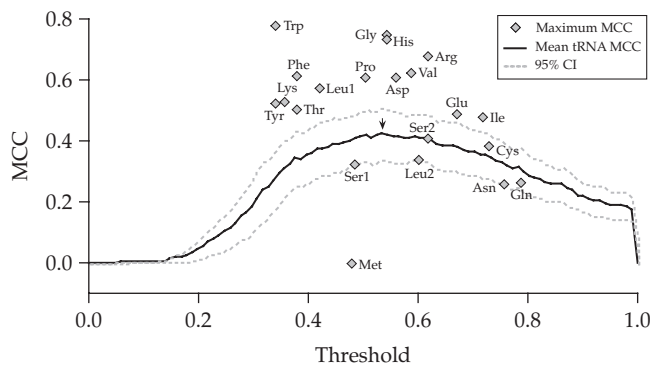


Figure 6.7 Mathew's correlation coefficient (MCC) for the 21 mammalian tRNAs. The mean value for all 21 tRNAs is shown as the black line with the 95% confidence interval (CI) is shown by dashed lines. The arrow indicates the point at which the mean MCC is maximized.

6.6 Software

Few user-friendly software packages have been written that generalize the mutational mapping method to different kinds of data (molecular and morphological) and a wide variety of biological questions. We introduce one such package, SIMMAP, which provides researchers with the ability to address a wide variety of questions using either molecular or morphological data. Briefly, SIMMAP is a software implementation of the indirect method of mapping mutational histories described in the first sections of this chapter. For example, SIMMAP can be used to sample character histories on phylogenies to address questions about general evolutionary patterns of change (trends), positive selection at focal sites or across a gene region, and correlation among characters (as described above), and will generate the raw mutational histories for custom analyses not available in the software package. In addition, SIMMAP can be used to calculate the posterior distribution of ancestral states in either a full hierarchical or empirical Bayesian framework. The software accommodates a wide variety of substitution models and priors. SIMMAP is free for academic use and a download can be obtained at www.simmmap.com.

6.7 Acknowledgments

We would like to acknowledge the following funding agencies for support during the writing: a Danish FSS grant (271050599) to J.P.B and R. N, and a Carlsberg Foundation grant (21000680) to P.P.G.

References

- Adkins, R.M. and Honeycutt, R.L. (1994) Evolution of the primate cytochrome c oxidase subunit II gene. *J. Mol. Evol.* **38**: 215–231.
- Bishop, J.G., Dean, A.M., and Mitchell-Olds, T. (2000) Rapid evolution of plant chitinases: molecular targets of selection in plant-pathogen coevolution. *Proc. Natl. Acad. Sci. USA* **97**: 5322–5327.
- Bollback, J.P. (2002) Bayesian model adequacy and choice in phylogenetics. *Mol. Biol. Evol.* **19**: 1171–1180.
- Bollback, J.P. (2006) SIMMAP: stochastic character mapping of discrete traits on phylogenies. *BMC Bioinformatics* **7**: 88.
- Brooks, D.R. and McLennan, D.A. (1991) *Phylogeny, Ecology, and Behavior: a Research Program in Comparative Biology*. University of Chicago Press, Chicago.
- Chiu, D.K. and Kolodziejczak, T. (1991) Inferring consensus structure from nucleic acid sequences. *Comput. Appl. Biosci.* **7**: 347–352.
- Dimmic, M.W., Hubisz, M.J., Bustamante, C.D., and Nielsen, R. (2005) Detecting coevolving amino acid sites using bayesian mutational mapping. *Bioinformatics* **21** (suppl. 1): i126–i135.
- Felsenstein, J. (1985) Phylogenies and the comparative method. *Am. Nat.* **125**: 1–15.
- Gillespie, J. (1991) *The Causes of Molecular Evolution*. Oxford University Press, Oxford.
- Gutell, R.R., Power, A., Hertz, G.Z., Putz, E.J., and Stormo, G.D. (1992) Identifying constraints on the high order structure of RNA: continued development and application of comparative sequence analysis methods. *Nucleic Acids Res.* **20**: 5785–5795.
- Harvey, P.H. and Pagel, M.D. (1991) *The Comparative Method in Evolutionary Biology*. Oxford University Press, Oxford.
- Huelsenbeck, J.P. and Ronquist, F. (2001) MRBAYES: Bayesian inference of phylogenetic trees. *Bioinformatics Applications Note* **17**: 754–755.
- Huelsenbeck, J.P., Nielsen, R., and Bollback, J.P. (2003) Stochastic mapping of morphological characters. *Syst. Biol.* **52**: 131–158.
- Koshi, J.M. and Goldstein, R.A. (1996) Probabilistic reconstruction of ancestral protein sequences. *J. Mol. Evol.* **42**: 313–320.
- Krogh, A., Larsson, B., von Heijne, G., and Sonnhammer, E.L. (2001) Predicting transmembrane protein topology with a hidden Markov model: application to complete genomes. *J. Mol. Biol.* **305**: 567–580.
- Kyte, J. and Doolittle, R.F. (1982) A simple method for displaying the hydropathic character of a protein. *J. Mol. Biol.* **157**: 105–132.
- Lanavé, C., Preparata, G., Saccone, C., and Serio, G. (1984) A new method for calculating evolutionary substitution rates. *J. Mol. Evol.* **20**: 86–93.
- Langley, C.H. and Fitch, W.M. (1974) An estimation of the constancy of the rate of molecular evolution. *J. Mol. Evol.* **3**: 161–177.
- Messier, W. and Stewart, C.-B. (1997) Episodic adaptive evolution of primate lysozymes. *Nature* **385**: 151–154.
- Mummidi, S., Bamshad, M., Ahuja, S.S., Gonzalez, E., Feuillet, P.M., Begum, K. et al. (2000) Evolution of human and non-human primate cc chemokine receptor 5 gene and mRNA. Potential roles for haplotype and

- mRNA diversity, differential haplotype specific transcriptional activity, and altered transcription factor binding to polymorphic nucleotides in the pathogenesis of HIV-1 and simian immunodeficiency virus. *J. Biol. Chem.* **275**: 18946–18961.
- Nielsen, R. (2001) Mutations as missing data: inferences on the ages and distributions of nonsynonymous and synonymous mutations. *Genetics* **159**: 401–411.
- Nielsen, R. (2002) Mapping mutations on phylogenies. *Syst. Biol.* **51**: 729–732.
- Nielsen, R. and Huelsenbeck, J.P. (2001) Detecting positively selected amino acid sites using posterior predictive p-values. In *Pacific Symposium on Biocomputing Proceedings*, pp. 576–588. World Scientific, Singapore.
- Pagel, M.D. (1999) Inferring the historical patterns of biological evolution. *Nature* **401**: 877–884.
- Paterlini, M.G. (2002) Structure modeling of the chemokine receptor CCR5: implications for ligand binding and selectivity. *Biophys. J.* **83**: 3012–3031.
- Pupko, T., Pe'er, I., Shamir, R., and Graur, D. (2000) A fast algorithm for joint reconstruction of ancestral amino acid sequences. *Mol. Biol. Evol.* **17**: 890–896.
- Robinson, D.M., Jones, D.T., Kishino, H., Goldman, N., and Thorne, J.L. (2003) Protein evolution with dependence among codons due to tertiary structure. *Mol. Biol. Evol.* **20**: 1692–1704.
- Suchard, M.A., Weiss, R.E., Sinsheimer, J.S., Dorman, K.S., Patel, P., and McCabe, E.R.B. (2003) Evolutionary similarity among genes. *J. Am. Stat. Assoc. Theory Methods* **98**: 653–662.
- Templeton, A.R. (1996) Contingency tests of neutrality using intra/interspecific gene trees: the rejection of neutrality for the evolution of the cytochrome oxidase II gene in the hominoid primates. *Genetics* **144**: 1263–1270.
- Yang, Z. (1994) Maximum likelihood phylogenetic estimation from DNA sequences with variable rates over sites: approximate methods. *J. Mol. Evol.* **39**: 306–314.
- Yang, Z., Kumar, S., and Nei, M. (1995) A new method of inference of ancestral nucleotide and amino acid sequences. *Genetics* **141**: 1641–1650.
- Yoder, A.D. and Yang, Z. (2004) Divergence dates for Malagasy lemurs estimated from multiple gene loci: geological and evolutionary context. *Mol. Ecol.* **13**: 757–773.
- Yu, J. and Thorne, J.L. (2006) Dependence among sites in RNA evolution. *Mol. Biol. Evol.* **23**: 1525–1537.